TÜBİTAK

Original Article

Turk J Med Sci
2012; 42 (Sup.2): 1519-1527

E-mail: medsci@tubitak.gov.tr
doi:10.3906/sag-1203-12

Effect of intravitreal octreotide acetate injection on retinal neovascularization, morphology, and apoptotic cell death in an oxygen-induced retinopathy mouse model

Fatma Selin KAYA[1], İmren AKKOYUN[1], Asuman Nihan HABERAL REYHAN[2], Attila DAĞDEVİREN[3], Gürsel YILMAZ[1], Sibel OTO[1], Yonca AKOVA[1]

Aim: To investigate the effect of octreotide acetate on neovascularization, retinal structures, and apoptotic cell death in an oxygen-induced retinopathy (OIR) mouse model.

Materials and methods: A total of 26 C57BL/6J mice were exposed to 75 ± 2% oxygen from postnatal day 7 to 12. On day 12, 12 mice (group C) were injected with 0.1 µg intravitreal octreotide acetate (IVOA) and 14 mice (group D) were injected with 0.05 µg IVOA, in the right eye. The contralateral eyes were injected with 1 µL isotonic saline (control group, group B). Four mice were used as negative controls (group A). Neovascularization was quantified by counting the number of retinal vascular endothelial cell nuclei anterior to the inner limiting membrane. Structural changes were examined by light and electron microscopy. Apoptosis was investigated using the TUNEL technique.

Results: The retinal vascular endothelial cell nuclei count was lower in groups C ($P < 0.0001$) and D ($P < 0.0001$) compared with group B. Light microscopy showed no retinal toxicity. Electron microscopy showed mitochondrial damage in the inner segment of the photoreceptors in the OIR mouse model without increasing in the IVOA-injected groups. There was no significant difference in the apoptotic cell death in any of the groups.

Conclusion: There was mitochondrial damage in the inner segment of the photoreceptors in the OIR mouse model without increasing the apoptotic cell death.

Key words: Oxygen-induced retinopathy mouse model, neovascular ocular diseases, apoptosis, mitochondria, octreotide acetate

Introduction

Pathologic retinal angiogenesis is a final common pathway leading to vision loss in neovascular ocular diseases such as retinopathy of prematurity, diabetic retinopathy, and age-related macular degeneration (1–3). Vascularization requires a complex series of cellular events that are initiated and modulated by various growth factors (4,5). Vascular endothelial growth factor (VEGF) has been localized to both retinal cells and microvascular endothelium (2,6). Although the vascular bed and distribution of tissue disease varies across these ocular neovascular diseases, the proliferation of aberrant blood vessels is common to all (2,3,7,8). Drugs that inhibit the biological activity of VEGF or the insulin-like growth factor-1 (IGF-1) axis represent a new paradigm in the treatment of intraocular neovascular diseases. The currently used anti-VEGF drugs are pegaptanib, ranibizumab, and bevacizumab. Somatostatin, also known as the growth hormone-inhibiting hormone,

Received: 04.03.2012 – Accepted: 30.05.2012
[1] Department of Ophthalmology, Faculty of Medicine, Başkent University, Ankara – TURKEY
[2] Department of Pathology, Faculty of Medicine, Başkent University, Ankara – TURKEY
[3] Department of Histology and Embryology, Faculty of Medicine, Başkent University, Ankara – TURKEY
Correspondence: *İmren AKKOYUN, Department of Ophthalmology, Faculty of Medicine, Başkent University, 06490 Bahçelievler, Ankara – TURKEY*
E-mail: retina95akk@yahoo.de

has an antiangiogenic effect (4,5,9). Inhibition of angiogenesis in proliferative retinopathies using somatostatin analogs has been investigated (10,13). Systemic therapy with somatostatin analog octreotide was described to result in the regression of neovascularization (14). Somatostatin and its receptors are promising candidates for such an action (15). Systemic therapy with somatostatin analog octreotide was described recently in the clinical trials of diabetic retinopathy treatments, but with conflicting results (11,13,15,16).

In the present study, we investigated the effects of intravitreal octreotide acetate (IVOA) injection on retinal neovascularization at 2 different concentrations, evaluated the drug-related morphological and ultrastructural changes using light microscopy (LM) and electron microscopy (EM), and determined apoptotic cell death in a well-established oxygen-induced retinopathy (OIR) mouse model using C57BL/6J mice (7). The OIR in the mouse, with vascular development similar to that in human and reproducible and quantifiable proliferative retinal neovascularization, is useful for the study of the pathogenesis of retinal neovascularization, as well as for the study of medical intervention for retinal vasculopathies (6).

Materials and methods

All of the animals were treated in accordance with the Association for Research in Vision and Ophthalmology Statement for the Use of Animals in Ophthalmic and Vision Research. The animal procedures were approved by the local Animal Care and Use Committee of Başkent University.

Experimental protocol

We used a murine model of OIR that was described previously and in which retinal neovascularization is induced reproducibly (7). Briefly, on postnatal day (P) 7, C57BL/6J mice were placed in a hyperoxic chamber (75 ± 2% oxygen) for 5 days with their nursing mothers. On P12, the mice were removed from the chamber and placed in room air (21% oxygen). A commercially available solution of octreotide acetate (Novartis, USA) was used. The octreotide acetate was obtained directly from a vial of octreotide acetate, undiluted from its solvent vehicle. During the experiment, we used the doses of 0.1 μg and 0.05 μg. For the 0.1 μg octreotide acetate injection, 1 μL of the original suspension was injected. For the 0.05 μg octreotide acetate injection, 1.0 mL of the original solution was diluted with 1.0 mL sterile saline, whereupon 1 μL of the new solution was immediately injected into the vitreous cavity. The mice were deeply anesthetized using an intraperitoneal injection of ketamine hydrochloride (40 mg/kg) and xylazine hydrochloride (5 mg/mL). Additionally, the eye was desensitized with a drop of 0.5% proparacaine hydrochloride. Intravitreal injections were performed on P12 with a 32-gauge needle and Hamilton syringe under direct observation with a stereoscopic microscope, at the corneoscleral junction, at the 6 o'clock position. The right eye received an intravitreal injection of 1 μL octreotide acetate and the left eye received 1 μL of isotonic saline (NaCl) in the same position. Four mice of the same age that had been kept in room air, without exposure to high levels of oxygen, served as the negative controls. On P17, the mice were killed using an intraperitoneal injection of ketamine hydrochloride (100 mg/kg) and xylazine hydrochloride (5 mg/mL), and the eyes were enucleated.

A total of 26 C57BL/6J mice were exposed to 75 ± 2% oxygen from P7 to P12. On day 12, 12 mice (group C, n = 12 eyes) were injected with 0.1 μg IVOA and 14 mice (group D, n = 14 eyes) were injected with 0.05 μg IVOA, in the right eye. The contralateral eyes were injected with isotonic saline (control group, group B, n = 26 eyes). Four age-matched mice, maintained in room air, were used as the negative controls (negative control, group A, n = 8 eyes). The enucleated eyes were examined by LM (in groups A, B, C, and D, 5, 23, 9, and 11 eyes, respectively) and EM (3 eyes in each group). The extent of apoptosis was investigated using the terminal deoxynucleotidyl transferase-mediated dUTP nick end labeling (TUNEL) technique. TUNEL staining was performed using paraffin sections, which were used for LM (in group A, 5 eyes; in groups B, C, and D, 6 eyes in each group).

Light microscopy

The enucleated eyes were fixed with 4% formalin and embedded in paraffin for light microscopic evaluation. Serial sections of the retina (6 μm thick) were obtained starting from the optic disk. The second or third sections after the optic disk were taken for evaluation. One section per eye was evaluated. For the

quantitative assessment of retinal neovascularization, periodic acid–Schiff and hematoxylin-stained serial sections were used. Neovascularization was quantified by counting the number of retinal vascular endothelial cell nuclei anterior to the inner limiting membrane (ILM) per histological section of the retina. In the morphological analysis of retinal layers, findings such as cystic degeneration, hypocellularity, or loss of the nuclear layer were investigated specifically for each group. The slides were examined using LM (OLYMPUS BX51, Germany).

Electron microscopy

For the electron microscopic examination, all of the tissues were fixed in phosphate buffer containing 2.5% glutaraldehyde for 2–3 h. Next, they were postfixed in 1% osmium tetroxide (OsO_4) and dehydrated in a series of graded alcohols. After passing through propylene oxide, the specimens were embedded in Araldite CY212, 2-dodecenyl succinic anhydride (DDSA), benzyl dimethyl amine (BDMA), and dibutyl phthalate. Semithin sections were cut and stained with toluidine blue and examined with a light microscope. Ultrathin sections were stained with uranyl acetate and lead citrate and examined with a LEO 906E EM transmission electron microscope. Evaluation of the ultrastructural morphology, especially of the inner and outer photoreceptor layers, was performed in each group using EM.

The EM and LM assessments of the retinal tissues were performed by 2 independent observers in a blinded fashion.

The TUNEL technique

The enucleated globes were fixed in 4% paraformaldehyde and embedded in paraffin. Serial sections of the retina (6 μm thick) were obtained, starting from the optic disk. The third or fourth sections after the optic disk were taken for evaluation and stained with hematoxylin and eosin. One section per eye was evaluated. TUNEL staining was performed with a kit (In Situ Cell Death Detection Kit, AP, Roche Diagnostics GmbH, Mannheim, Germany) according to the manufacturer's instructions. Two independent observers were used in blinded-fashion LM to look for TUNEL-positive cells in randomly selected fields on each slide and at 100× magnifications (oil immersion). Apoptotic TUNEL-positive cells were counted in 10 randomly selected fields on each slide.

Statistical analyses

The results are reported as means ± standard deviations (SDs). One-way analysis of variance (Statistica 10.0, StatSoft Inc., Tulsa, Oklahoma, USA) was performed on all of the documented parameters. The independent variables were experimental conditions (groups A, B, C, D). As results, P-values are reported in the Figures. In cases of an overall significant difference ($P < 0.05$), Duncan's post hoc test was used to identify differences among any of the 4 groups (groups A–D). $P < 0.05$ indicated significant differences. Figures were plotted using IBM SPSS Statistics Release 19.0.0.1 (IBM Corporation, Armonk, New York, USA).

Results

Quantification of proliferative retinopathy with and without IVOA injection

The degree of hyperoxia-induced neovascularization was quantified in serial paraffin sections by counting the endothelial cell nuclei on the vitreal side of the ILM. In group B (control group), the retina contained multiple neovascular tufts extending into the vitreous (Figure 1). These tufts originated from the retinal vessels, forming clusters of immature endothelial cells. In this group, the mean ± SD of the endothelial nuclei anterior to the ILM was 19.9 ± 2.6 per

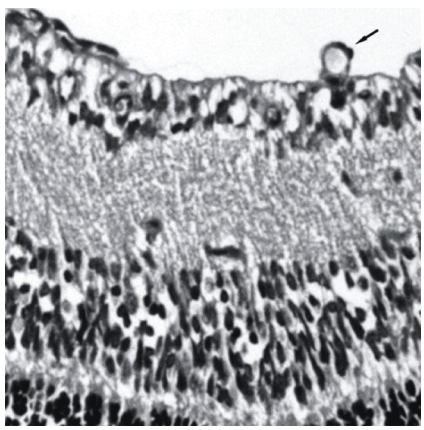

Figure 1. Light micrographs of C57BL/6J mice retina. Group B = control group; arrow indicates neovascular tuft extending into the vitreous. Original magnification 20×.

histological section. The endothelial cell nuclei count was 5.1 ± 1.0 in group C (0.1 μg IVOA) and 6.9 ± 1.4 in group D (0.05 μg IVOA). Groups C ($P < 0.0001$) and D ($P = 0.0001$) displayed significant differences compared with group B, the control group. There was no significant difference between groups C and D ($P = 0.23$). Significant differences were obtained when group A was compared with groups B, C, and D ($P < 0.0001$) (Figure 2). Compared with the control group (group B), the endothelial cell nuclei counts were reduced by 75% in group C (0.1 μg IVOA) and 65% in group D (0.05 μg IVOA).

Morphological analysis using light microscopy

There were no morphological changes such as cystic degeneration, hypocellularity, and losses in the photoreceptor cell layer using LM evaluation in any of the groups (Figure 3).

Ultrastructural analysis using electron microscopy

The evaluation of the ultrathin sections revealed no distinguishable sign of morphological changes in the negative control group (group A), including mitochondria in the inner segment of the photoreceptors (Figure 4). In the control group (group B), there were some changes in the morphology of mitochondria, seen as a mottled matrix and electron-dense bodies in the central region of the cristae surrounded by a lytic matrix and cristalysis in the inner segment of the photoreceptors (Figure 5). These ultrastructural changes were also detectable in IVOA-injected groups C and D. To quantify the mitochondrial dysmorphology in the groups, we defined an atypical mitochondrion with a mottled matrix and electron-dense bodies in the central region of the cristae and extensive cristalysis, and we counted the numbers of these in the fields of view using the same magnification (3250×) for each sample in the given area for each group. The results are given in Figure 6. Regarding the atypical mitochondria counts, groups B, C, and D, when compared with the negative control group, displayed significant differences ($P < 0.0001$). There was no significant difference between groups C and D when compared with the control group ($P = 0.09$ and $P = 0.16$, respectively). There was no significant difference between groups C and D ($P = 0.08$).

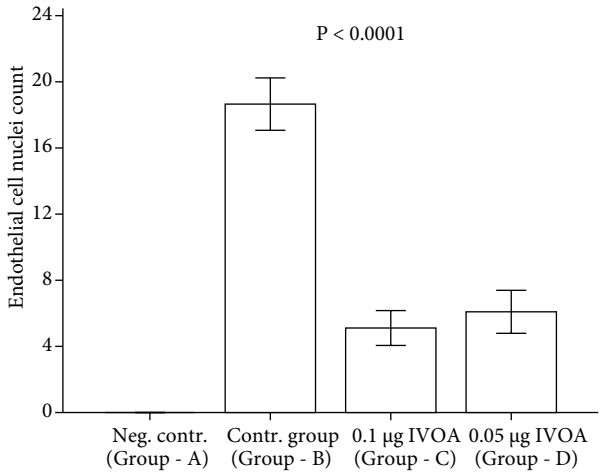

Figure 2. Histogram showing the count of neovascular cell nuclei on the vitreal side of the inner limiting membrane of the retina in the OIR model with C57BL/6J mice in different study groups. Mean ± SD values are the results of analysis of variance (ANOVA) and denote differences by experiment (groups A–D).

Apoptosis analysis with the TUNEL technique

For each sample, the number of TUNEL-positive cells was determined. In the negative control group, the control group, and the IVOA-injected groups, we detected apoptotic TUNEL-positive cells in the outer nuclear layer and the inner nuclear layer, without a significant difference between the groups (Figures 7 and 8). There was no significant difference when group A was compared with groups B ($P = 0.8$), C ($P = 0.7$), or D ($P = 0.6$). No significant difference was seen when group B was compared with groups C ($P = 0.9$) or D ($P = 0.8$). There was no difference between groups C and D ($P = 0.7$).

Discussion

In the present study, using a well-established OIR mouse model with C57BL/6J mice, we observed the effect of intravitreally injected octreotide acetate on retinal endothelial cell proliferation and the effect on retinal structures and apoptosis with different octreotide acetate concentrations.

We demonstrated a dose-independent decrease in the retinal endothelial cell count with intravitreal injections of 0.05 μg and 0.1 μg octreotide acetate. This finding suggests that octreotide acetate may have an antiangiogenic effect on retinal endothelial cell proliferation. The octreotide acetate potently

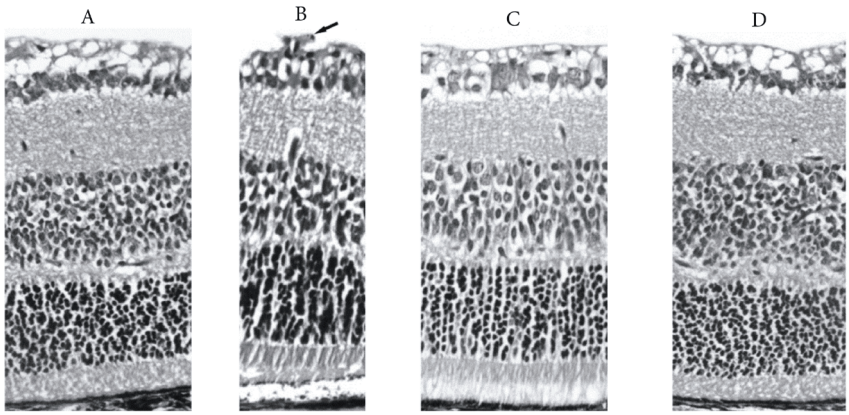

Figure 3. Light micrographs of C57BL/6J mice retina. The sections were taken from almost the same region of the retina in all of the groups. A) Mouse retina exposed to room air (group A, negative control group); B) isotonic saline-injected eye, exposed to hyperoxia from P7 to P12 (group B, control group; the arrow indicates endothelial cell proliferation; C) eye injected with 0.1 μg IVOA (group C); D) eye injected with 0.05 μg IVOA (group D). Original magnification 20×.

inhibited proliferation of bovine retinal endothelial cells induced with basic fibroblast growth factor (bFGF), VEGF, and IGF-1 under hypoxic conditions (18). Woltering et al. used the octreotide dosages of 0.5 μg, 2.5 μg, and 50 μg to inhibit angiogenesis in the chick disk and they observed inhibition rates of 15%, 56%, and 61%, respectively (19).

Smith et al. reported that in transgenic mice expressing a growth hormone antagonist gene and subjected to OIR, retinal neovascularization was reduced by 34% (20). Some in vivo studies demonstrated suppression of retinal revascularization in an OIR model using C57BL/6J mice (17,21). They reported a neovascularization suppression rate of 26% after an intraperitoneal injection of octreotide at a dose of 20 mg/kg twice a day (17). In another study, it was reported that intraperitoneal injections of octreotide acetate twice a day failed to inhibit neovascularization in a rat model of retinopathy of prematurity, although pharmacological serum octreotide levels were achieved (22). In our study, after intravitreal injection of octreotide acetate, we

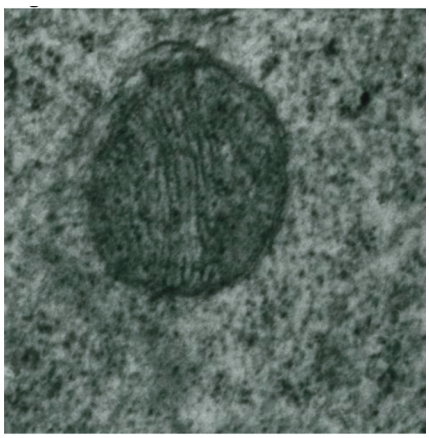

Figure 4. Electron micrograph: a section through the inner segments of photoreceptor cells (negative control group, group A). Mitochondrion reflects the usual fine structural characteristics.

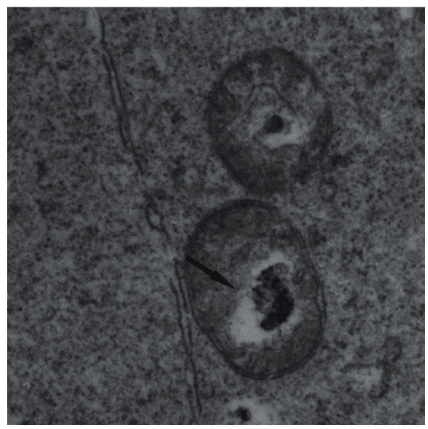

Figure 5. Electron micrograph: group B = control group. Morphological changes in the mitochondria as mottled matrix and electron-dense bodies in the central region of cristae surrounded by lytic matrix and extensive cristalysis.

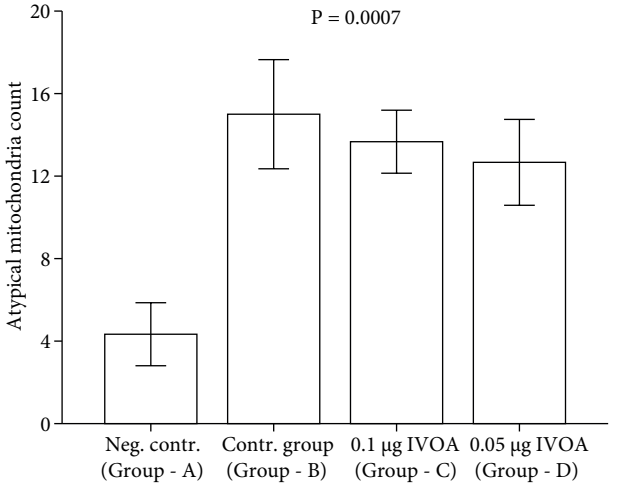

Figure 6. Histogram showing the number of atypical mitochondria in different study groups in the retina of C57BL/6J mice using an experimental model of oxygen-induced retinopathy. Mean ± SD values are the results of analysis of variance (ANOVA) and denote differences by experiment (groups A–D).

observed a suppression rate of 65% in the 0.05 µg IVOA group and 75% in the 0.1 µg IVOA group in an OIR mouse model with C57BL/6J mice. It was shown in C57BL/6J mice that somatostatin receptor-2 (SSTR2) is the main mediator of the ocular antiangiogenic procedures (23). The peptide octreotide does not cross the blood–brain barrier and would have access only where there is a disruption of the blood–retinal barrier, limiting the amount of drug reaching the retinal target tissue when injected subcutaneously (23). This could explain the higher dose requirements of systemic octreotide therapy. In vitro antiangiogenic activity of somatostatin agonists indicates a paracrine mechanism of action. Thus, the therapeutic effects of the octreotide are hypothesized to be mediated by somatostatin receptor activation directly on the ocular target tissue (23–25). McCombe et al. suggested that somatostatin analogs may act at the retinal level to inhibit the activity of growth hormone and IGF-1 locally, rather than at the level of the pituitary (26). These angioinhibitory effects, initiated by SSTR2 activation, involve the downregulation of VEGF. The signal transducer and activator of transcription 3 (stat3) is the downstream effector mediating this antiangiogenic action (25). These findings support the assumption that octreotide may be efficient via local administration and are consistent with the high neovascularization suppression rate in the present study.

It has been found that octreotide injected intravitreally in New Zealand white rabbit eyes was safe at dosages of 1 mg or less (27). In our study, octreotide acetate did not cause morphological changes in LM in layers of the retina in eyes with pigmented tissue in C57BL/6J mice in an OIR model treated with 0.1 µg and 0.05 µg IVOA.

It is well known that in OIR, hyperoxia deprivation induces relative hypoxia in the tissue (2), and this provokes swelling, fragmentation of the cristae, condensation of the matrix, and fading of the outer and inner membranes of the mitochondria (28,29). In accordance with the literature, in our control group (group B), which represents the OIR group without octreotide acetate, in the ultrastructural morphological investigation using EM, there was a mottled matrix and electron-dense bodies in the central region of the cristae surrounded by a lytic matrix and extensive cristalysis, maintaining the mitochondrial configuration in the outer borders in the inner segment of the photoreceptors. These findings, visible in the hyperoxia-exposed control group, indicate hyperoxia vulnerability of the C57BL/6J retina.

The internal structures of the mitochondria can change in response to their physiological state and reaction to a stress signal, such as exposure to hyper- or hypoxia (30). The level of stress seems to determine the morphological and functional changes in the mitochondria. These changes can induce the survival of the cell or lead to apoptosis (31). Using TUNEL staining, we detected apoptosis in the negative control group and in the control group, without a significant increase in apoptotic cell death in the OIR group (control group) as demonstrated in a previous study (32). Furthermore, we detected apoptosis in the IVOA-injected groups without a significant increase in apoptotic cell death compared with the OIR group and control group. Apoptosis occurs normally in many physiological processes and serves to eliminate harmful or unnecessary cells. Death by apoptosis is also responsible for the loss of cells in a variety of pathologic states, such as hypoxia or cytotoxic agents (33). In our study, we detected a physiological apoptotic process and no toxic effect of IVOA at concentrations of 0.1 µg and 0.05 µg

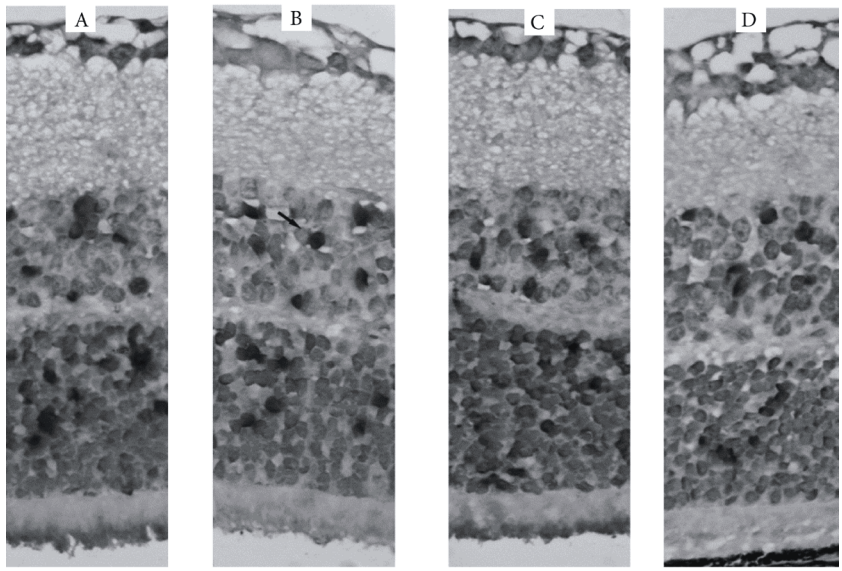

Figure 7. Light micrographs of C57BL/6J mice retina showing assessed apoptotic cells using TUNEL assay. Each slide represents the 5 independent experiments in groups A–D. Apoptotic cells are deeply pigmented (arrow) in the outer nuclear layer and inner nuclear layer in each group. Original magnification 100×, oil immersion.

octreotide in an OIR mouse model as examined by TUNEL staining.

In conclusion, our study demonstrated that an intravitreal injection of octreotide acetate suppresses endothelial cell proliferation in an OIR mouse model using C57BL/6J mice. LM did not show retinal toxicity in any of the groups. The electron microscopic cytoarchitectonic evaluation revealed mitochondrial damage in the inner segment of the photoreceptors in OIR without an increase in the IVOA-injected groups. There was no increasing apoptotic cell death in the IVOA-injected groups. The study described herein implies that an intravitreal injection of octreotide acetate may be a potential treatment for proliferative retinopathies. Further studies are needed to determine the safety and efficacy of somatostatin analogs in neovascular ocular diseases.

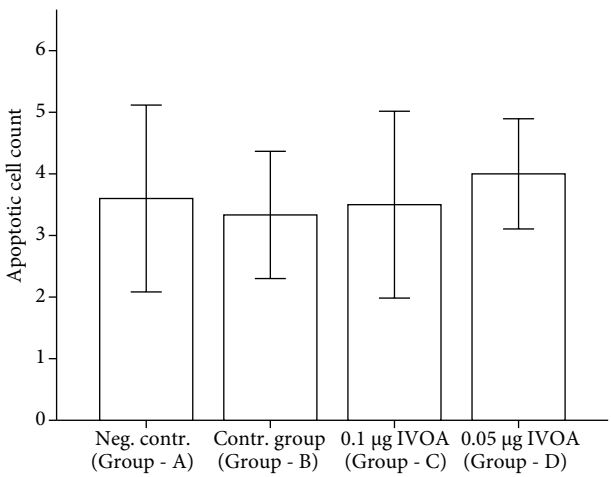

Figure 8. Histogram showing the count of detected apoptotic cells in different study groups in the retina of C57BL/6J mice using an experimental model of oxygen-induced retinopathy. Mean ± SD values are the results of analysis of variance (ANOVA) and denote differences by experiment (groups A–D).

Acknowledgment

The abstract of this manuscript was accepted as a free paper for EVER-2011/Crete – Greece.

This work was supported by the Research Fund of Başkent University, Ankara, Turkey.

We are indebted to İ. Vardarlı, MD, EU MSc (Epidemiology), Diabetes Center, Bad Lauterberg, Germany, for critical review of the manuscript and support in the statistical analyses.

References

1. Gibson DL, Sheps SB, Uh SH, Schechter MT, McCormick AQ. Retinopathy of prematurity-induced blindness: birth weight-specific survival and the new epidemic. Pediatrics 1990; 86: 405–12.
2. Pierce EA, Foley ED, Smith LE. Regulation of vascular endothelial growth factor by oxygen in a model of retinopathy of prematurity. Arch Ophthalmol 1996; 114: 1219–28.
3. Zimmer-Galler IE, Bressler NM, Bressler SB. Treatment of choroidal neovascularization: updated information from recent macular photocoagulation study group reports. Int Ophthalmol Clin 1995; 35: 37–57.
4. Battegay EJ. Angiogenesis: mechanistic insights, neovascular diseases, and therapeutic prospects. J Mol Med (Berl) 1995; 73: 333–46.
5. D'Amore PA. Mechanisms of retinal and choroidal neovascularization. Invest Ophthalmol Vis Sci 1994; 35: 3974–9.
6. Dündar S, Özcura F, Meteoğlu İ, Kara ME. Effects of long-term passive smoking on the vascular endothelial growth factor and apoptosis marker expression in the retina and choroid: an experimental study. Turk J Med Sci 2012; 42: 377–83.
7. Smith LE, Wesolowski E, McLellan A, Kostyk SK, D'Amato R, Sullivan R et al. Oxygen-induced retinopathy in the mouse. Invest Ophthalmol Vis Sci 1994; 35: 101–11.
8. Yan Q, Li Y, Hendrickson A, Sage EH. Regulation of retinal capillary cells by basic fibroblast growth factor, vascular endothelial growth factor, and hypoxia. In Vitro Cell Dev Biol Anim 2001; 37: 45–9.
9. Gragoudas ES, Adamis AP, Cunningham ET Jr, Feinsod M, Guyer DR. Pegaptanib for neovascular age-related macular degeneration. N Engl J Med 2004; 351: 2805–16.
10. Dal Monte M, Ristori C, Cammalleri M, Bagnoli P. Effects of somatostatin analogues on retinal angiogenesis in a mouse model of oxygen-induced retinopathy: involvement of the somatostatin receptor subtype 2. Invest Ophthalmol Vis Sci 2009; 50: 3596–606.
11. Grant MB, Caballero S Jr. The potential role of octreotide in the treatment of diabetic retinopathy. Treat Endocrinol 2005; 4: 199–203.
12. Palii SS, Caballero S Jr, Shapiro G, Grant MB. Medical treatment of diabetic retinopathy with somatostatin analogues. Expert Opin Investig Drugs 2007; 16: 73–82.
13. Vasilaki A, Thermos K. Somatostatin analogues as therapeutics in retinal disease. Pharmacol Ther 2009; 122: 324–33.
14. Missotten T, Baarsma GS, Kuijpers RW, van den Born LI, van der Loos T, Croxen R et al. Somatostatin-related therapeutics in ophthalmology: a review. J Endocrinol Invest 2005; 28: 118–26.
15. Boehm BO, Lang GK, Jehle PM, Feldman B, Lang GE. Octreotide reduces vitreous hemorrhage and loss of visual acuity risk in patients with high-risk proliferative diabetic retinopathy. Horm Metab Res 2001; 33: 300–6.
16. Grant MB, Mames RN, Fitzgerald C, Hazariwala KM, Cooper-DeHoff R, Caballero S et al. The efficacy of octreotide in the therapy of severe nonproliferative and early proliferative diabetic retinopathy: a randomized controlled study. Diabetes Care 2000; 23: 504–9.
17. Higgins RD, Yan Y, Schrier BK. Somatostatin analogs inhibit neonatal retinal neovascularization. Exp Eye Res 2002; 74: 553–9.
18. Baldysiak-Figiel A, Lang GK, Kampmeier J, Lang GE. Octreotide prevents growth factor-induced proliferation of bovine retinal endothelial cells under hypoxia. J Endocrinol 2004; 180: 417–24.
19. Woltering EA, Barrie R, O'Dorisio TM, Arce D, Ure T, Cramer A et al. Somatostatin analogues inhibit angiogenesis in the chick chorioallantoic membrane. J Surg Res 1991; 50: 245–51.
20. Smith LE, Kopchick JJ, Chen W, Knapp J, Kinose F, Daley D et al. Essential role of growth hormone in ischemia-induced retinal neovascularization. Science 1997; 276: 1706–9.
21. Wilkinson-Berka JL, Lofthouse S, Jaworski K, Ninkovic S, Tachas G, Wraight CJ. An antisense oligonucleotide targeting the growth hormone receptor inhibits neovascularization in a mouse model of retinopathy. Mol Vis 2007; 13: 1529–38.
22. Averbukh E, Halpert M, Yanko R, Yanko L, Peèr J, Levinger S et al. Octreotide, a somatostatin analogue, fails to inhibit hypoxia-induced retinal neovascularization in the neonatal rat. Int J Exp Diabetes Res 2000; 1: 39–47.
23. Palii SS, Afzal A, Shaw LC, Pan H, Caballero S, Miller RC et al. Nonpeptide somatostatin receptor agonists specifically target ocular neovascularization via the somatostatin type 2 receptor. Invest Ophthalmol Vis Sci 2008; 49: 5094–102.
24. Dal Monte M, Cammalleri M, Martini D, Casini G, Bagnoli P. Antiangiogenic role of somatostatin receptor 2 in a model of hypoxia-induced neovascularization in the retina: results from transgenic mice. Invest Ophthalmol Vis Sci 2007; 48: 3480–9.
25. Dal Monte M, Ristori C, Videau C, Loudes C, Martini D, Casini G et al. Expression, localization, and functional coupling of the somatostatin receptor subtype 2 in a mouse model of oxygen-induced retinopathy. Invest Ophthalmol Vis Sci 2010; 51: 1848–56.
26. McCombe M, Lightman S, Eckland DJ, Hamilton AM, Lightman SL. Effect of a long-acting somatostatin analogue (BIM23014) on proliferative diabetic retinopathy: a pilot study. Eye (Lond) 1991; 5: 569–75.
27. Liang C, Peyman GA, Conway MD, Woltering EA. Retinal toxicity of intravitreous octreotide in the rabbit. Can J Ophthalmol 1997; 32: 229–32.

28. Benninghoff A, Dreckhahn D. Anatomie. Munich: Urban & Fischer; 2008.

29. Natoli R, Provis J, Valter K, Stone J. Expression and role of the early-response gene Oxr1 in the hyperoxia-challenged mouse retina. Invest Ophthalmol Vis Sci 2008; 49: 4561–7.

30. Benítez-Bribiesca L, Gómez-Camarillo M, Castellanos-Juárez E, Mravko E, Sánchez-Suárez P. Morphologic, biochemical and molecular mitochondrial changes during reperfusion phase following brief renal ischemia. Ann N Y Acad Sci 2000; 926: 165–79.

31. Detmer SA, Chan DC. Functions and dysfunctions of mitochondrial dynamics. Nat Rev Mol Cell Biol 2007; 8: 870–9.

32. Akkoyun I, Karabay G, Haberal N, Dagdeviren A, Yilmaz G, Oto S et al. Structural consequences after intravitreal bevacizumab injection without increasing apoptotic cell death in a retinopathy of prematurity mouse model. Acta Ophthalmol 2012; 90: 564–70.

33. Vinay K, Abul K, Nelson F, Stanley L, Ramzi S. Robbins & Cotran pathologic basis of disease. Philadelphia (PA): Saunders Publishing; 2005.